ANNEALING EFFECT ON VIBRATION MODES OF ALUMINUM NITRIDE THIN FILMS

EFECTO DEL TRATAMIENTO TÉRMICO EN MODOS VIBRACIONALES DE PELÍCULAS DELGADAS DE NITRURO DE ALUMINIO

Roberto Bernal-Correa[†], Mario E. Rodríguez-García[‡], Álvaro Pulzara-Mora[†]

[†]Laboratorio de Nanoestructuras Semiconductoras. Grupo de Magnetismo y Materiales Avanzados Universidad Nacional de Colombia, sede Manizales, Colombia A.A. 127.
[‡]Centro de Física Aplicada y Tecnología Avanzada, Departamento de Nanotecnología, Universidad Nacional Autónoma de México, Campus Juriquilla, Querétaro, Qro, México.

(Recibido: Abril/2014. Aceptado: Junio/2014)

Abstract

Reactive magnetron sputtering was used to prepare aluminum nitride (AlN) films at an intermediate substrate temperature of 450 ^{o}C. In order to analyze the microstructure and vibrational phonon modes of Al_xN_y and Al_mO_n clusters, the sample was subjected to thermal annealing in a controlled nitrogen atmosphere at temperatures of 550 ^{o}C and 650 ^{o}C, for 20 minutes. The morphological surface was studied by scanning electron microscopy (SEM), and allows us to determine the size, geometry and the facets formation of AlN crystals. The change of microstructure from wurtzite-AlN as-prepared cubic-AlN annealing samples is discussed. From Fourier transform infrared spectroscopy (FTIR) measurements in the range of 650 to 2000 cm^{-1}, the phonon frequencies of Al_xN_y and Al_mO_n clusters were obtained. The experimental frequencies were compared to theoretical calculations by using density Functional theory (DFT).

Keywords: Aluminum nitride, Magnetron sputtering, FT-IR.

Roberto Bernal-Correa: rabernalco@unal.edu.co

Resumen

Películas de nitruro de aluminio (AlN) fueron obtenidas por magnetrón sputtering a una temperatura de sustrato intermedia de 450 ^{o}C, con el fin de analizar la microestructura y modos fononicos vibracionales de los grupos Al_xN_y y Al_mO_n. La muestra se sometió a un tratamiento térmico en una atmósfera de nitrógeno controlado a temperaturas de 550 ^{o}C y 650 ^{o}C, durante 20 minutos. La morfología de la superficie se estudió mediante microscopía electrónica de barrido (SEM), permitiendo determinar el tamaño, la geometría y la formación de cristales de AlN. Se discute el cambio de la microestructura de wurtzita-AlN a cúbico-AlN después de realizado el tratamiento térmico. Medidas de espectroscopia infrarroja con transformada de Fourier (FTIR) en el rango de 650 a 2000 cm^{-1}, permitieron obtener frecuencias asociadas a modos vibracionales de clústeres de Al_xN_y Al_mO_n. Las frecuencias experimentales se compararon con cálculos teóricos realizados mediante el uso de la teoría de densidad funcional (DFT).

Palabras clave: Nitruro de aluminio, Magnetrón sputtering, FT-IR.

Introduction

In the last decade, the study of thin films and methods used to prepare them, have been the subject of research due to its wide field of applications. Some of the most widely studied materials for the production of semiconductor films are the family III-N, as GaN, InN and AlN.[1–3] These semiconductor alloys are important in the fabrication of optical devices that emit light in the blue and UV range for applications in optoelectronics.[4, 5] Aluminum nitride (AlN) is the largest band gap semiconductor (6.2 eV for the wurtzite, and 5.9 eV for the zincblende cubic phase).[6] AlN hexagonal phase (α-AlN), is generally grown by using high-cost techniques as metal organic chemical vapor deposition (MOCVD), molecular beam epitaxy (MBE), or laser ablation (LA). The other hand, the Zincblende (β-AlN) phase is very difficult to crystallize,

and only a few reports of their physical properties are known.[7, 8] β-AlN is mainly used as a buffer layer for growth GaN and ZnO.[9] Other methods to prepare α-AlN polycrystalline are CVD, and different sputtering configurations using a Ar/N mixture as sputter gas at low working pressure, $\sim 10^{-2}$ Torr.[10, 11] In this case, the β-AlN and α-AlN phases can coexist, due to a defect that can originate during growth.[12]

Only a few theoretical and experimental studies have been performed in order to determine the most stable configuration, and the vibrational frequencies of small aluminum nitride Al_xN_y clusters. Other reports include, study of bonding of Al_nN (with n¡6) clusters by using first principles,[13] and a theoretical calculation of Al_3N^- and Al_4N^- using density functional theory.[14] The electronic properties and chemical bonding of Al_xN^- clusters by using ab initio calculation has been reported by B. Boris et al [15].

In the present work, we have carried out a detailed study of the vibration phonon modes obtained from FTIR spectra of a AlN-sample prepared at temperature of 450 ^{o}C by magnetron sputtering, which was subsequently subjected to a thermal annealing in nitrogen-argon continuous flow at temperatures of 550 ^{o}C and 650 ^{o}C, respectively. The morphological obtained from SEM images was used to relate to the optical properties of the samples with the size, and geometry of the AlN microcrystal's. Finally, experimental phonon frequencies of Al_xN_y and Al_mO_n clusters obtained from FTIR measurements were compared to the theoretical calculation using density functional theory (DFT).

Experimental

Thin films of AlN were deposited by the r.f. reactive magnetron sputtering (MS) technique on a glass substrate in an Argon-Nitrogen mixture atmosphere, using an Al target (2 inch diameter 1.25 inch thick, 99.99% purity) and high purity nitrogen gas. Substrates were rinsed in acetone, and ultrasonic cleaned before being placed into the chamber. The background

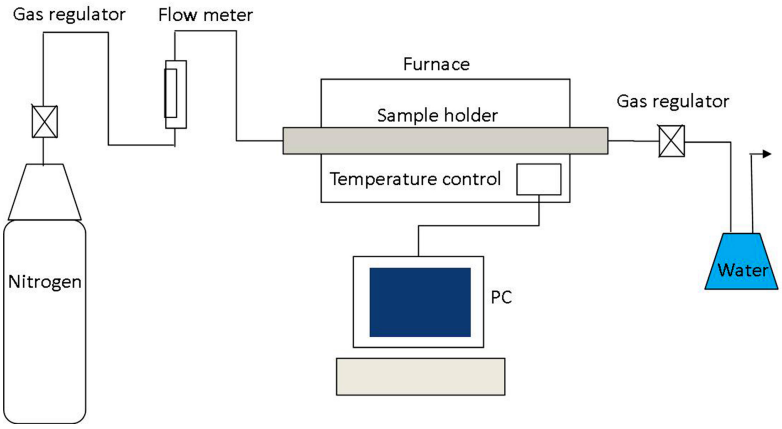

FIGURE 1. *Experimental setup of the thermal treatment of the AlN films.*

pressure into the chamber was at 1×10^{-6}Torr. Previously, to deposit the AlN layer, a buffer layer of Al (100 nm thickness) was deposited on a glass substrate in an Argon atmosphere ($P_{Ar} = 2 \times 10^{-2}$ Torr). The input of nitrogen and argon gases into the chamber was controlled by an individual needle valve, which able maintaining a pressure ratio constant ($P_{Ar}/P_N = 2$). Time deposition and working pressure were fixed at one hour and 10^{-3}Torr, respectively. After growth, the film was subsequently subjected to annealing in a continuous flow of nitrogen. The high temperature furnace (thermolyne-21100) equipped with a gas flow meter and temperature controller was used to perform the heating annealing (Fig. 1). The thermal annealing procedure is described as follows: After inserting the Al/AlN films into the quartz tube, the post-annealing was then carried out at two different temperatures: 550 ^{o}C and 650 ^{o}C respectively. The heating rate was 10 ^{o}C/min, and the annealing time was 20 minutes.

Scanning electron microscopy is used to analysis the microstructure of the aluminum nitride samples. Scanning electron microscopy images were taken in plan view in a 1 μm scale, in different magnifications. Before taking the SEM images, and to prevent the accumulation of static electric fields at the sample, a gold ultra-thin coating was deposited on the sample by using a low vacuum

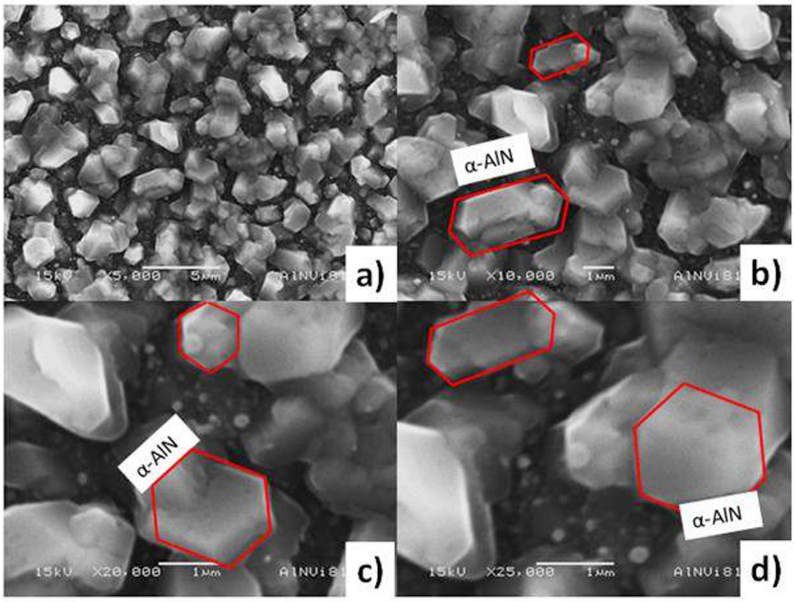

FIGURE 2. *Plan-view SEM images of the as-prepared AlN film at substrate temperature of 450 °C. a) ×5000, b) ×10000, c) ×20000 and d) ×25000 magnifications. The golden lines illustrated the possible micro-crystals' shapes.*

sputter. The FT-IR absorbance measurements were performed in the 650–2000 cm^{-1} frequency range by using a bruker vector 33 spectrophotometer which supplies an FT–IR microscope operating in absorbance mode, with a resolution of less than 1 cm^{-1} and unpolarized light at near normal incidence.

Results

I. Scanning Electron Microscopy (SEM)

Figure 2, shows a plan-view scanning electron micrographs with magnification of (a) ×5000, (b) ×10000, (c) ×20000 and (d) ×25000 of as-prepared AlN sample at temperature of 450 °C. In this figure, the bottom layer in each microphotograph corresponds to the Al buffer layer. The crystals are scattered on Al buffer layer deposited on a glass substrate. In these images, the formation of tilted micro–crystals of hexagonal shape with different facets is observed. The thickness of thin film is about 1 μm, and the

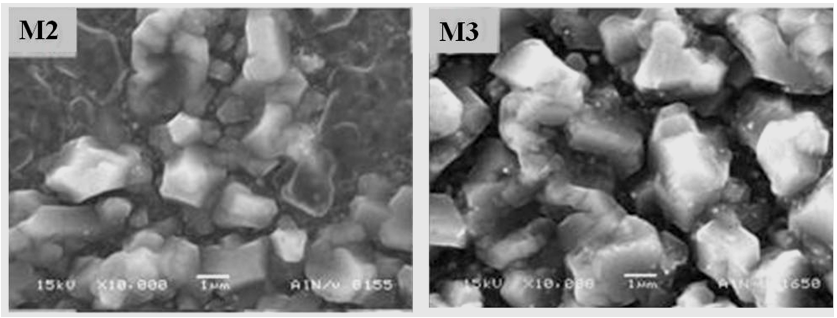

FIGURE 3. *SEM images of the AlN samples after a thermal annealing at temperatures of 550 °C (M2) and 650 °C (M3).*

size of the AlN crystallites vary from 1 to 2 μm. Some hexagonal micro crystals exhibit facets along of (0001), (10–10), (1–100), and (1–2–10) crystallographic directions. One possible reason of this behavior is the large difference in the thermal expansion coefficient between Al – AlN and Si used as substrate, which produce a strong stress in the sample. However, the shape and orientation of the microcrystal's may be related to the deposition angle α (off-normal deposition), because it provides an asymmetry on an impingement flux. The effects of the deposition angle (α) on structural, shape and orientation of the AlN single crystal have been studied in detail by R. Deng et al. [16], Y. Xu et al. [17], and Y. Sato et al. [18].

For samples subject to thermal annealing, we saw that some crystals are detached of the substrate letting an imprint of the crystallite shape on it (Fig. 3-M2). Crystal shape changes from hexagonal to cubic suggesting that a phase transformation is presenting. One possible reason to explain this behavior is the huge quantity of oxygen incorporated into the AlN during heat treatment. As the oxygen is incorporated into AlN lattice promote the formation of Al vacancies which are very effective in scattering the phonons, resulting in a decrease the thermal conductivity [19, 20]. The grain boundary phonon scattering can also affect the thermal conductivity.

According to EDS spectrum of the M2) and M3) AlN samples,

reveal that our samples contain O, and N as elements constituent, which can promote not only formation of Al-N and Al-O chains but also vibration modes relating to AlN and AlO. It is well known that the impurities or defects (e.g. oxygen in AlN) in the crystal lattice decrease the thermal constant, but increase the thermal stress. The thermal conductivity in polycrystalline samples can reduce by either the random orientation of the individual crystals, or the random discrete distribution of the secondary phase. Slack et al, have studied the changes in the thermal conductivity as a function of the oxygen content.[21] He found that for a sample nearly free of impurities and defects, the thermal conductivity is $\sim$3.5 $Wcm^{-1}K^{-1}$ at room-temperature, while those containing oxygen impurities have a lower thermal conductivity.[22]

II. FT-IR Measurements

In order to analyze the phonons scattering concerning to N and O impurities in AlN, we carried out measurements of FTIR - diffuse reflectance spectra near normal incidence from 800 cm^{-1} to 2000 cm^{-1} for the as-prepared (M1) and thermal annealed samples (M2-M3). To understand the experimental result, note that according to our experimental configuration the E_1(TO) mode is excited by an electric field perpendicular to the c-axis of the wurzite unit cell, while the E_1(TO) mode is excited by electric field parallel to the c-axis. This means that, if our FTIR spectra were measured using normal incidence, the electric field was parallel to the sample surface or parallel to the micro-crystals orientation according to SEM images (Fig. 2 and 3). Then, only an intense E_1(TO) band and a very weak A_1(TO) band should be observed. However, because our samples are polycrystalline with preferential oriented along (111) direction, both E_1(TO) and A_1(TO) phonon modes must appear, because the selection rule is broken.

It is well known that wurtzite-AlN present only characteristic E_1(LO) or A_1(TO) active IR phonons modes at 672 cm^{-1}. The A_1 and E_1 (LO) phonon modes near 910 cm^{-1}, and E_2 mode at 665 cm^{-1} is alone IR inactive, and come from Brillouin zone center (k=0) phonons,[23] as shown in Fig. 4-M1. In the spectrum of

as-prepared sample a strong Reststrahlen (Rt) band from 870 cm^{-1} to 1000 cm^{-1} is also seen clearly.[24] This Rt band is very sensible to phonon absorption of the micro-crystals and surface roughness. Absorption peak at 1972 cm^{-1} labeled by an arrow-up probably come from a C impurity because it is a very common impurity in AlN prepared by sputtering.

On the other hand, the introduction of impurities (substitution or interstitially) into the lattice host destroy the translational symmetry of the wave vector, and additional infrared vibration phonon modes can be activated. The perturbation of the lattice by substitution impurity is a change in the mass of the one of the constituents and a modification of the bonding forces. If the impurity is much lighter than the host atom it replaces then high frequency vibration mode above ω_{TO} appears. These vibration amplitudes are localized near the impurity and hence are known as local vibration modes (LVM). For heavier impurities, the impurity-related vibrations can occur within the phonon band or in the gap between the acoustic and optical bands. These modes are referred to as resonant modes (RM) or gap modes (GM). Raman phonon modes of AlN cluster are very difficult to predict, because, they present discrete absorptions spectra, and depend on the geometry configuration.

FTIR spectra of the samples with thermal annealing (TA) at temperatures of 550 ^{o}C (M2) and 650 ^{o}C (M3) are shown in the Fig. 4, M2) and M3), contrasted with that from an (M1) as-prepared sample. Combined effects of stress and alloying generate the blue shift observed in the absorption Reststrahlen edge for as-prepared samples. A slight distortion in the line shape of the Reststrahlen band is observed, but the depth of the Rt band decreases when thermal annealing increases. The top of the Reststrahlen band is strongly distorted, conceivably caused by the roughness of the surface, grain boundaries, and size of the micro crystals, as seen in the (M2-M3)-SEM images of Fig. 3. These results demonstrate that the variation of the top of the Reststrahlen band can be attributed to the effects of surface

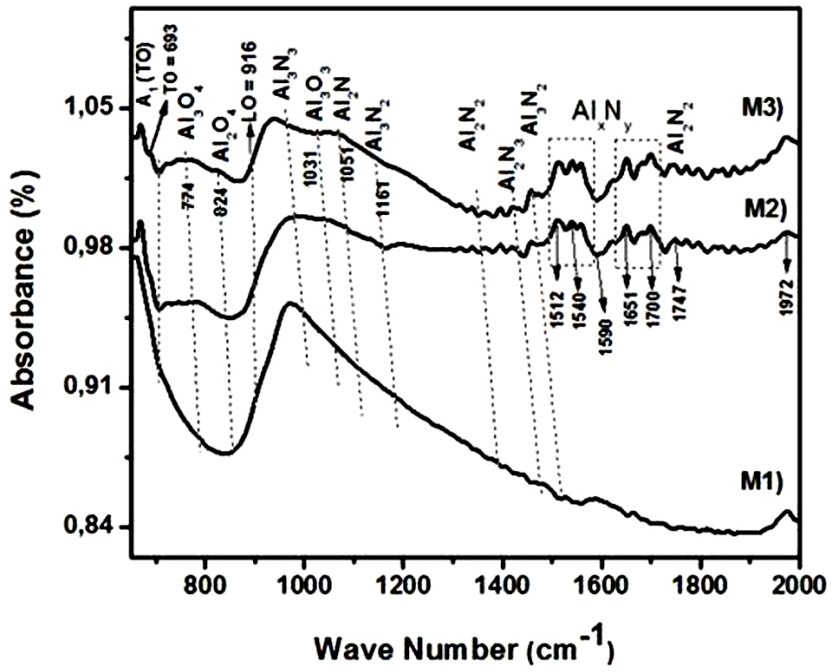

FIGURE 4. *M1) Absorbance spectrum of the as-prepared AlN sample at 450 °C. The samples M2) and M3) were subjected to thermal annealing in a nitrogen atmosphere at temperatures of 550 °C and 650 °C, respectively.*

disorder in the samples, and it reflects the microstructure of the films. In the FTIR-spectra several pits are evident up to (1200 $\text{cm}^{-1} \leq k \leq 1900\ \text{cm}^{-1}$) and below (600 $\text{cm}^{-1} \leq k \leq 890\ \text{cm}^{-1}$) of the Reststrahlen region, owing to the formation of Al_xN_y and Al_mO_n complex. The high affinity of AIN with O, can promote the formation of intermediate phases between $(\text{AIN})_m$ and complex of Al_mO_n (s≠2, n≠3), contributing to the scattering of phonons in this region. Nearness of the thermal annealing temperature (TA = 600 °C) of the melting temperature (Tm = 650 °C) of Al, may be the cause of some of the micro-crystals were detached from the surface samples, affecting the vibration phonon modes relating to Al_xN_y and Al_mO_n clusters in this FTIR region. In the range of 1200 cm^{-1} to 1600 cm^{-1} over the continuous FTIR spectra emerge a series of peaks associated to vibration phonons modes of chain-clusters of Al_xN_y. The phonon modes of Al_xN_y

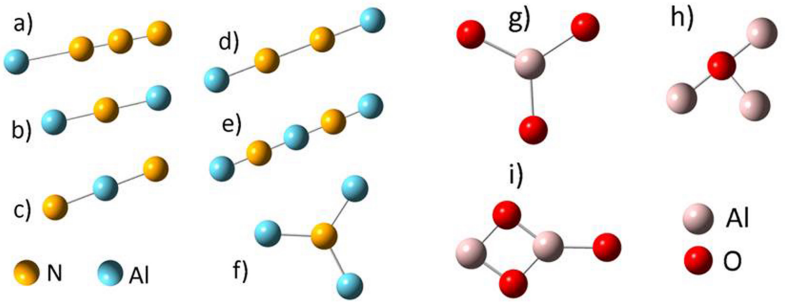

FIGURE 5. *Geometric arrangements of clusters of Al_xN_y and Al_mO_n. a) AlNNN, b) Al_2N, c) AlN_2, d) Al_2N_2, e) Al_3N_2 and f) Al_3N, g) AlO_3, h) Al_3O, and i) Al_2O_3.*

and Al_mO_n complex chains are not easily identifiable, because they generally depend on geometrical configuration, and it is necessary to carry out theoretical calculations to compare the vibration modes calculated for a particular structure with experiments.

III. DFT Calculations

In order to identify some vibration bands in the FTIR spectra, we carried out theoretical calculations through the density functional theory (DFT), employing the hybrid B3LYP functional with help of the Gaussian program.[25] In Table 1, we have listed the geometries distance and vibration frequencies (cm^{-1}) of the clusters used in our theoretical calculations. Some configurations of the AlN-chains used in this work are presented in Fig. 5.

According to theoretical results, we found that most of the frequencies associated with Al_mO_n clusters are below the Reststrahlen band, while that the vibration frequencies (cm^{-1}) corresponding to Al_xN_y clusters are larger than the Reststrahlen band. From FTIR experimental spectrum, we identified the following vibration bands relating to Al_mO_n clusters: Al_3O (611), Al_2O_2 (720.3), Al_2O_3 (750), and AlO_2 (780), Al_2O_4 (824), Al_3O_4 (774), AlO_3 (1001), and Al_3O_3 (1031). A.B.C Patzer et al. has reported that some of these structures have planar geometries alternating Al and O atoms. Moreover, all stables species of Al_mO_n comply with the m/n stoichiometry ratio.[26, 27]

Clusters	Distance (Å)	Geometry	Frequencies (cm^{-1})-Intensities (IR, Raman)
$\mathbf{Al_2N}$	Al-N = 1.731	$(^2\Sigma_u^+)$	133.3(23.67,0), 525.4(0, 11.13), 1052.4(86.14, 0)
$\mathbf{Al_3N_2}$	Al-N = 1.705 N-Al = 1.713	$(^2\Sigma_u^+)$	42.4(6.97, 0), 154.0(29.53,0), 376.4(0, 83.17), 675.9(201.19, 0), 1166.3(1098,0), 1167.3(0, 166.68)
$\mathbf{AlN_2}$	Al-N = 1.804	$(^4\Pi_u)$	157.2(53.9, 0), 163.9(81.1, 0), 646.2(0, 706), 660.1(1036, 0)
AlNNN	Al-N = 1.826 N-N = 1.206 N-N = 1.138	$(^1\Sigma^+)$	97.1(0.85, 7.38), 496.4(141, 42.3), 627.0(21.2, 0.89), 627.8(21.2, 0.89), 1463.3(277.8,0.26), 2266.9(850,48.7)
$\mathbf{AlN_2Al}$	Al-N = 1.888 N-N = 1.204	$(^3\Sigma_g^+)$	73.2(4.4,0.2), 209.6(0.1, 19.26), 332(8.7, 676), 606(341.6, 10.67), 1744(7.9, 5878)
$\mathbf{Al_3N}$	Al-N = 1.850	(D_{3h})	156.3(3.8, 5.1), 223.62(0.2, 0), 427.52(0,56.9), 749.44(326.4, 0.10), 749.46(326.4,0.11)
$\mathbf{Al_3O}$	Al-O = 1.977 O-Al = 1.854	(C_{2v})	135(1.3, 3.3), 157(2.1, 24.4), 186(3.6, 1.9), 297(24.1, 109.1), 433(8.5, 37.15), 611(49.06, 90.5)
$\mathbf{AlO_3}$	Al-O = 1.623 O-Al = 1.881	(C_{2v})	175(0.3,2), 466(2.1, 9), 560(6.48, 14.12), 1001(52.8,23.6), 1013(20.4, 63.68)
$\mathbf{Al_2O_3}$	Al-O = 1.750 Al-O = 1.764 O-Al = 1.788	(C_{2v})	200(0.1, 10.8), 226(16.7, 3.8), 290(87.2, 1.4), 451(2.37, 51.37), 606(33.6, 8.6), 629(11.5, 1), 673(30.9, 22), 750(92.8, 1.7), 858(76.2, 8.13)

TABLE 1. *Optimized geometries used in the theoretical calculations in this work obtained by DFT - B3LYP/cc-pVDZ, for a set of Al_xN_y and Al_mO_n chain-clusters.*

On the other hand, the experimental IR-bands Al_3N_3 (870), Al_2N (1051), Al_3N_2 (1161), Al_2N_3 (1350), Al_3N_2 (1477), AlN_3 (1463), Al_2N_3 (1500), and Al_2N_2 (1747), were identified as upper Reststrahlen bands, as indicated in Fig. 4, and are consistent with our theoretical calculation. These results show that, the frequencies larger than the Reststrahlen band are related to either symmetric or antisymetric stretching modes of Al-N bond, in agreement with the theoretical results reporter by other authors.[28, 29]

Conclusions

The morphology studied of AlN films by SEM showed the facets formations. The change of their microstructure is related to

a transformation of phase from wurtzite-AlN to be cubic-AlN after annealing. FTIR measurements also showed evidence of the formation of Al_xN_y, Al_xO_y clusters, whose vibration frequencies are in good agreement with theoretical calculations using DTF.

Acknowledgments

This work was partially supported by DIMA. R. A. Bernal-Correa thanks to COLCIENCIAS for scholarship "Francisco Jose de Caldas" and Facultad de Minas - Universidad Nacional de Colombia, sede Medellin.

References

[1] X. Jiao, Y. Shi, H. Zhong, R. Zhang, and J. Yang, J. Mater. Sci.-Mater. El. , 1 (2014).

[2] J. Kim and Y. Cho, J. Korean Phys. Soc. **64**, 994 (2014).

[3] X.-M. Cai, Y.-Q. Hao, D.-P. Zhang, and P. Fan, Appl. Surf. Sci. **256**, 43 (2009).

[4] S. Adachi, *Properties of Group-IV, III-V and II-VI Semiconductors*, Wiley Series in Materials for Electronic & Optoelectronic Applications (Wiley, 2005).

[5] F. Randriamora, J. Bruyere, and A. Deneuville, Mater. Sci. Eng. B-Adv. **50**, 272 (1997).

[6] H. Morkoc, S. Strite, G. B. Gao, M. E. Lin, B. Sverdlov, and M. Burns, J. Appl. Phys. **76**, 1363 (1994).

[7] T. Yoshitake, S. Mohri, T. Hara, and K. Nagayama, Jpn. J. Appl. Phys. **47**, 3600 (2008).

[8] R. Thapa, B. Saha, and K. Chattopadhyay, J. Alloys Compd. **475**, 373 (2009).

[9] K. Sumitani, R. Ohtani, T. Yoshida, Y. Nakagawa, S. Mohri, and T. Yoshitake, Jpn. J. Appl. Phys. **49**, 020212 (2010).

[10] C. R. Aita, J. Appl. Phys. **53**, 1807 (1982).

[11] M. Garcia-Mendes, S. Morales-Rodriguez, R. Machorro, and W. De la Cruz, Rev. Mex. Fis. **54**, 271 (2008).

[12] O. Ambacher, J. Phys. D: Appl. Phys. **31**, 2653 (1998).

[13] S. Nayak, B. Rao, P. Jena, X. Li, and L.-S. Wang, Chem. Phys. Lett. **301**, 379 (1999).

[14] Li, X. and Wang, L.-S., Eur. Phys. J. D **34**, 9 (2005).

[15] B. B. Averkiev, A. I. Boldyrev, X. Li, and L.-S. Wang, J. Chem. Phys. **125**, 124305 (2006).

[16] R. Deng, P. Muralt, and D. Gall, J. Vac. Sci. Technol. A **30**, 051501 (2012).

[17] Y. Xu, C. H. Lei, B. Ma, H. Evans, H. Efstathiadis, M. Rane, M. Massey, U. Balachandran, and R. Bhattacharya, Supercond. Sci. Technol. **19**, 835 (2006).

[18] Y. Sato, K. Matsuo, Y. Takahashi, K. Muranaka, K. Fujino, S. Hahakura, K. Ohmatsu, and H. Takei, IEEE Trans. Appl. Supercond. **11**, 3365 (2001).

[19] V. Ambegaokar, Phys. Rev. **114**, 488 (1959).

[20] M. Holland, Phys. Rev. **134**, A471 (1964).

[21] G. A. Slack, L. J. Schowalter, D. Morelli, and J. A. F. Jr., J. Cryst. Growth **246**, 287 (2002).

[22] G. A. Slack, R. Tanzilli, R. Pohl, and J. Vandersande, J. Phys. Chem. Solids **48**, 641 (1987).

[23] X. Li, C. Zhou, G. Jiang, and J. You, Mater. Charact. **57**, 105 (2006).

[24] M. Kazan, B. Ruffle, C. Zgheib, and P. Masri, J. Appl. Phys. **98**, 103529 (2005).

[25] L. Andrews, M. Zhou, G. V. Chertihin, W. D. Bare, and Y. Hannachi, J. Phys. Chem. A **104**, 1656 (2000).

[26] Patzer, A. B.C., Chang, Ch., Sedlmayr, E., and Sulzle, D., Eur. Phys. J. D **32**, 329 (2005).

[27] C. Chang, A. Patzer, E. Sedlmayr, T. Steinke, and D. Snulzle, Chem. Phys. Lett. **324**, 108 (2000).

[28] A. Costales, A. K. Kandalam, and R. Pandey, J. Phys. Chem. B **107**, 4508 (2003).

[29] A. Costales and R. Pandey, Chem. Phys. Lett. **362**, 210 (2002).